Matrix Isolation FTIR Spectroscopic and Density Functional Theoretical Studies of the Nickel, Copper, and Silver Carbonyl Chlorides

Limin Shao, Luning Zhang, Mingfei Zhou,* and Qizong Qin

Department of Chemistry, Laser Chemistry Institute, Fudan University, Shanghai, People's Republic of China

Received October 24, 2000

The nickel, copper, and silver metal carbonyl chloride molecules have been prepared and isolated in solid argon by cocondensation of the species generated from 1064 nm laser ablation of metal chlorides with carbon monoxide in excess argon at 11 K. On the basis of isotopic substitution experiments and density functional theory frequency calculations, infrared absorptions at 2118.7, 2156.8, and 2184.0 cm^{-1} are assigned to the C−O stretching vibrations of the Ni(CO)Cl, Cu(CO)Cl, and Ag(CO)Cl molecules. Density functional calculations predicted that the M(CO)Cl (M = Ni, Cu, Ag) molecules are linear; the binding energies with respect to MCl + CO were estimated to be 37.7, 34.2, and 17.8 kcal/mol, respectively. In addition, evidence is also presented for the $M(CO)Cl_2$, $M(CO)_2Cl$, and $M(CO)_2Cl_2$ (M = Ni, Cu) molecules.

Introduction

Transition-metal carbonyl complexes are cornerstones of modern coordination chemistry and organometallic chemistry.[1] Many industrial processes such as hydroformylation, Fischer−Tropsch synthesis, and acetic acid synthesis employ CO as the reagent and transition-metal compounds as heterogeneous or homogeneous catalysts and involve transition-metal carbonyl intermediates.[2] Transition-metal carbonyl halides have received attention for more than a century. In 1868, Schutzenberger succeeded in isolating and identifying the carbonyl chlorides of platinum with the compositions $Pt(CO)_2Cl_2$, $Pt_2(CO)_4Cl_4$, and $Pt_2(CO)_3Cl_4$.[3] Subsequently, carbonyl halides such as $Pd(CO)Cl_2$, Cu(CO)Cl, and Au(CO)Cl have been prepared and structurally characterized.[4−6]

Matrix isolation infrared spectroscopy has proved to be a highly effective method for characterization of transition-metal compounds with weakly bound ligands. The interactions of transition-metal halides such as difluorides and dichlorides of first-row transition metals with carbon monoxide in cryogenic matrices have been studied.[7,8] Some novel transition-metal carbonyl chlorides have been characterized by infrared and EXAFS spectroscopy.[9] The C−O stretching vibrational frequencies of these species shifted to high frequency of diatomic carbon monoxide.

In this paper, we report a study of combined matrix isolation FTIR spectroscopy and DFT studies on the complexes of nickel, copper, and silver chlorides with carbon monoxide generated from the reaction of laser-ablated nickel, copper, and silver chlorides with carbon monoxide molecules in excess argon.

Experimental and Theoretical Methods

The experimental setup for pulsed laser ablation and matrix infrared spectroscopic investigation is similar to that described previously.[10,11] The 1064 nm Nd:YAG laser fundamental (spectra Physic, DCR 2, 20 Hz repetition rate and 8 ns pulse width) was focused onto a rotating metal chloride target through a hole in a CsI window, Typically, 5−10 mJ/pulse laser power was used. The laser-ablated metal chlorides were codeposited with CO in excess argon onto a 11 K CsI window for 1 h at a rate of 2−4 mmol/h. The CsI window was mounted on a copper holder at the cold end of the cryostat (Air Products Displex DE202) and maintained by a closed-cycle helium refrigerator (Air Products Displex IR02W). A Bruker IFS 113v Fourier transform infrared spectrometer equipped with a DTGS detector was used to record the IR spectra in the range of 400−4000 cm^{-1} with a resolution of 0.5 cm^{-1}. Carbon monoxide, isotopic $^{13}C^{16}O$, and $^{12}C^{16}O + {}^{13}C^{16}O$ mixture samples were used in different experiments. Annealing experiments were done by warming the sample deposit to the desired temperature and quickly cooling to 11 K.

* To whom correspondence should be addressed. E-mail: mfzhou@fudan.edu.cn. Fax: +86-21-65102777.

(1) Cotton, F. A.; Wilkinson, G.; Murillo, C. A.; Bochmann, M. *Advanced Inorganic Chemistry*, 6th ed. Wiley: New York, 1999.

(2) See for example: Solomon, E. I.; Jones, P. M.; May, J. A. *Chem. Rev.* **1993**, *93*, 2623. Sen, A. *Acc. Chem. Res.* **1993**, *26*, 303. Vannice, M. A. *Catal. Today* **1992**, *12*, 255.

(3) Schutzenberger, P. *Bull. Soc. Chim. Fr.* **1868**, *10*, 188.

(4) Manchot, W.; Konig, J. *Chem. Ber.* **1926**, *59*, 883.

(5) Jones, P. J. *Z. Naturforsch.* **1982**, *B37*, 823. Browning, J.; Goggin, P. L.; Goodfellow, R. J.; Norton, M. G.; Rattray, A. J. M.; Taylor, B. F.; Mink, J. *J. Chem. Soc., Dalton Trans.* **1977**, 2061. Manchot, W.; Gail, H. *Chem. Ber.* **1925**, *58*, 2175.

(6) Hakansson, M.; Jagner, S. *Inorg. Chem.* **1990**, *29*, 5241. Hakansson, M.; Jagner, S.; Kettle, S. F. A. *Spectrochim. Acta* **1992**, *48A*, 1149. Plitt, H. S.; Bar, M. R.; Ahlrichs, R.; Schnockel, H. *Inorg. Chem.* **1992**, *31*, 463.

(7) DeKock, C. W.; Van Leirsburg, D. A. *J. Am. Chem. Soc.* **1972**, *94*, 3235.

(8) Van Leirsburg, D. A.; DeKock, C. W. *J. Phys. Chem.* **1974**, *78*, 134.

(9) Beattie, I. R.; Jones, P. J.; Young, N. A. *J. Am. Chem. Soc.* **1992**, *114*, 6146.

(10) Chen, M. H.; Wang, X. F.; Zhang, L. N.; Yu, M.; Qin, Q. Z. *Chem. Phys.* **1999**, *242*, 81.

(11) Chen. M. H.; Zhou, M. F.; Zhang, L. N.; Qin, Q. Z. *J. Phys. Chem. A* **2000**, *104*, 8627.

10.1021/om000911h CCC: $20.00
Publication on Web 02/16/2001

Density functional calculations were carried out using the Gaussian 98 program.[12] The three-parameter hybrid functional according to Becke with additional correlation corrections of Lee, Yang, and Parr were utilized (B3LYP).[13,14] Recent calculations have shown that this hybrid functional can provide very reliable predictions of the state energies, structures, and vibrational frequencies of transition-metal-containing compounds.[15−17] The 6-311+G(d) basis set was used for C, O, and Cl atoms, the all-electron basis sets of Wachters-Hay as modified by Gaussian were used for Ni and Cu atoms, and the Los Alamos ECP plus DZ basis set (LANL2DZ) was used for the Ag atom.[18−20] The geometries were fully optimized, vibrational frequencies were calculated with analytic second derivatives, and zero point vibrational energies were derived. The scaling factors of C−O stretching vibrations were determined as experimental observed frequency divided by calculated frequency.

Results

Infrared Spectra. Experiments were done using $NiCl_2$, $CuCl_2$, CuCl, and AgCl targets. Sample deposition at 11 K reveals strong CO absorption at 2138.4 cm^{-1} and ClCO absorptions at 1877.1 and 570.5 cm^{-1} that are common for all systems.[21] In addition, absorptions at 2154 and 2149.2 cm^{-1} due to CO perturbed by HCl and H_2O were always observed in the experiments.[22,23]

(a) $NiCl_2$ + CO/Ar. Experiments were done using a $NiCl_2$ target with different CO concentrations in argon (0.2% and 0.5%), and the product absorptions are listed in Table 1. The spectra in the 2200−2060 and 530−410 cm^{-1} regions with 0.5% CO in Ar which are of particular interest here are shown in Figure 1. One hour of sample deposition at 11 K produced strong $NiCl_2$ absorptions (520.9 cm^{-1} for $^{58}Ni^{35}Cl_2$)[24] and weak $Ni(CO)_x$ absorptions (not shown: NiCO, 1994.4 cm^{-1}; $Ni(CO)_2$, 1965.6 cm^{-1}; $Ni(CO)_3$, 2017.2 cm^{-1}; $Ni(CO)_4$, 2051.8 cm^{-1}).[25] The NiCl absorptions were hardly detected. New absorptions at 2190.2, 2118.7, 2126.6, 2075.0, and 469.1 cm^{-1} were produced on sample deposition. The 2190.2 and 2118.7 cm^{-1} bands decreased, while the 2126.6 and 2075.0 cm^{-1} bands increased on annealing. Sample annealing also produced new absorptions at 2148.4, 525.2, and 434.4 cm^{-1}. In an experiment at lower CO concentration (0.2%), the 2190.2, 2118.7, and 469.1 cm^{-1} bands were also observed after sample deposition and increased on 25 and 30 K annealing. The 2148.4, 2126.6, and 2075.1 cm^{-1} bands were only produced on annealing. Experiments were also done with isotopic-labeled ^{13}CO and mixed $^{12}CO + {}^{13}CO$ samples, and the spectra are shown in Figure 2.

(b) $CuCl_2$ + CO/Ar. The product absorptions from codeposition of laser-ablated $CuCl_2$ and CO/Ar mixture are listed in Table 2, and the spectra in the 2210−2120 and 540−410 cm^{-1} regions are shown in Figure 3. One hour of sample deposition produced strong $CuCl_2$ and CuCl absorptions[26] and weak $Cu(CO)_x$ (x = 1−3) ab-

Table 1. IR Absorption (cm^{-1}) from Codeposition of Laser-Ablated $NiCl_2$ with CO in Excess Argon at 11 K

$^{12}C^{16}O$	$^{13}C^{16}O$	R(12/13)	assignt
2190.2	2141.2	1.0229	$Ni(CO)Cl_2$
2149.2	2101.8	1.0226	H_2O-CO
2148.4	2101.2	1.0225	$Ni(CO)_2Cl_2$
2138.2	2091.1	1.0225	CO
2126.6	2078.5	1.0231	$Ni(CO)_2Cl$
2118.7	2069.9	1.0236	Ni(CO)Cl
2075.0	2029.1	1.0226	$Ni(CO)_2Cl$
2051.8	2005.4	1.0231	$Ni(CO)_4$
2017.2	1970.4	1.0238	$Ni(CO)_3$
1994.4	1946.5	1.0246	NiCO
1965.6	1921.3	1.0230	$Ni(CO)_2$
1877.1	1837.1	1.0218	ClCO
525.2			$^{58}Ni(CO)_2{}^{35}Cl_2$
520.9			$^{58}Ni^{35}Cl_2$
469.1			$^{58}Ni(CO)^{35}Cl_2$
434.4			$^{58}Ni(CO)_2{}^{35}Cl_2$

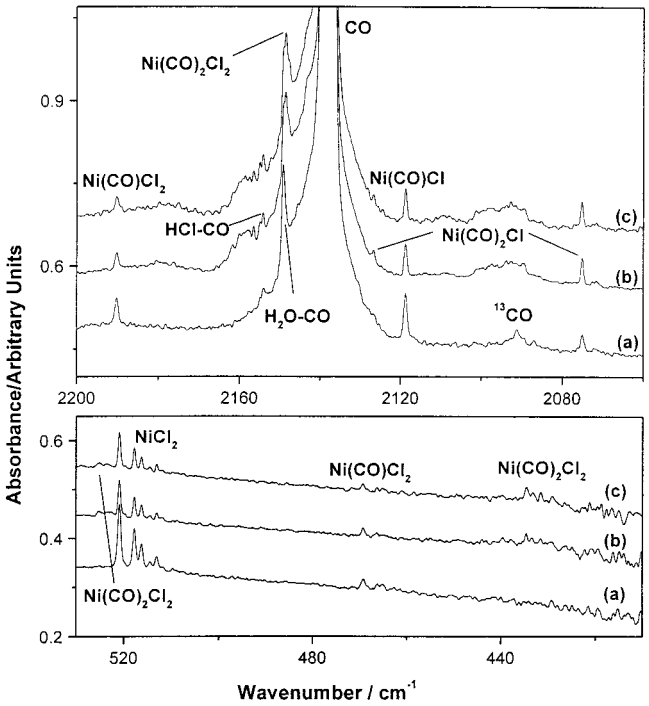

Figure 1. Infrared spectra in the 2200−2060 and 530−410 cm^{-1} regions from codeposition of laser-ablated $NiCl_2$ and 0.5% CO in argon: (a) 1 h sample deposition at 11 K; (b) after 25 K annealing; (c) after 30 K annealing.

(12) Frisch, M. J.; Trucks, G. W.; Schlegel, H. B.; Scuseria, G. E.; Robb, M. A.; Cheeseman, J. R.; Zakrzewski, V. G.; Montgomery, J. A., Jr.; Stratmann, R. E.; Burant, J. C.; Dapprich, S.; Millam, J. M.; Daniels, A. D.; Kudin, K. N.; Strain, M. C.; Farkas, O.; Tomasi, J.; Barone, V.; Cossi, M.; Cammi, R.; Mennucci, B.; Pomelli, C.; Adamo, C.; Clifford, S.; Ochterski, J.; Petersson, G. A.; Ayala, P. Y.; Cui, Q.; Morokuma, K.; Malick, D. K.; Rabuck, A. D.; Raghavachari, K.; Foresman, J. B.; Cioslowski, J.; Ortiz, J. V.; Stefanov, B. B.; Liu, G.; Liashenko, A.; Piskorz, P.; Komaromi, I.; Gomperts, R.; Martin, R. L.; Fox, D. J.; Keith, T.; Al-Laham, M. A.; Peng, C. Y.; Nanayakkara, A.; Gonzalez, C.; Challacombe, M.; Gill, P. M. W.; Johnson, B. G.; Chen, W.; Wong, M. W.; Andres, J. L.; Head-Gordon, M.; Replogle, E. S.; Pople, J. A. *Gaussian 98*, revision A.7; Gaussian, Inc.: Pittsburgh, PA, 1998.
(13) Becke, A. D. *J. Chem. Phys.* **1993**, *98*, 5648.
(14) Lee, C.; Yang, E.; Parr, R. G. *Phys. Rev. B* **1988**, *37*, 785.
(15) Bauschlicher, C. W., Jr.; Ricca, A.; Partridge, H.; Langhoff, S. R. In *Recent Advances in Density Functional Theory*; Chong, D. P., Ed.; World Scientific Publishing: Singapore, 1997; Part II.
(16) Bytheway, I.; Wong, M. W. *Chem. Phys. Lett.* **1998**, *282*, 219.
(17) Siegbahn, P. E. M. Electronic Structure Calculations for Molecules Containing Transition Metals. *Adv. Chem. Phys.* **1996**, *93*.
(18) McLean, A. D.; Chandler, G. S. *J. Chem. Phys.* **1980**, *72*, 5639. Krishnan, R.; Binkley, J. S.; Seeger, R.; Pople, J. A. *J. Chem. Phys.* **1980**, *72*, 650.
(19) Wachter, J. H. *J. Chem. Phys.* **1970**, *52*, 1033. Hay, P. J. *J. Chem. Phys.* **1977**, *66*, 4377.
(20) Hay, P. J.; Wadt, W. R. *J. Chem. Phys.* **1985**, *82*, 299.
(21) Jacox, M. E.; Milligan, D. E. *J. Chem. Phys.* **1965**, *43*, 866.
(22) Andrews, L.; Arlinghaus, R. T.; Johnson, G. L. *J. Chem. Phys.* **1983**, *78*, 6347.
(23) Dubost, H.; Abouaf-Marguin, L. *Chem. Phys. Lett.* **1972**, *17*, 269.
(24) Milligan, D. E.; Jacox, M. E.; McKinley, J. D. *J. Chem. Phys.* **1965**, *42*, 902.
(25) DeKock, R. L. *Inorg. Chem.* **1971**, *10*, 1205. Zhou, M. F.; Andrews, L. *J. Am. Chem. Soc.* **1998**, *120*, 11499.

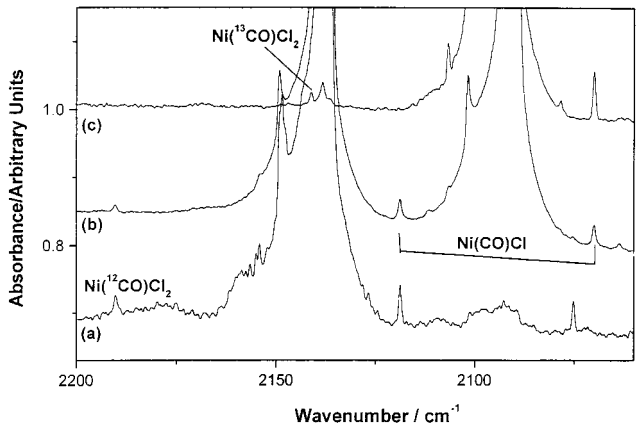

Figure 2. Infrared spectra in the 2200−2060 cm^{-1} region from codeposition of laser-ablated $NiCl_2$ and CO in excess argon: (a) 0.2% ^{12}CO, after 25 K annealing; (b) 0.4% ^{12}CO + 0.4% ^{13}CO, after 25 K annealing; (c) 0.5% ^{13}CO, after 25 K annealing.

Table 2. IR Absorption (cm^{-1}) from Codeposition of Laser-Ablated $CuCl_2$ with CO in Excess Argon

$^{12}C^{16}O$	$^{13}C^{16}O$	*R*(12/13)	assignt
2205.5	2156.0	1.0230	$Cu(CO)Cl_2$
2187.1			$Cu(CO)_2Cl_2$
2165.8	2116.7	1.0232	$Cu(CO)_2Cl$
2156.8	2107.3	1.0235	Cu(CO)Cl
2131.6	2084.4	1.0226	$Cu(CO)_2Cl$
2010.0	1965.8	1.0225	CuCO
1890.5	1847.0	1.0236	$Cu(CO)_2$
513.4			$^{63}Cu^{35}Cl_2$
459.1			$^{63}Cu(CO)^{35}Cl_2$
420.6			$^{63}Cu^{35}Cl$

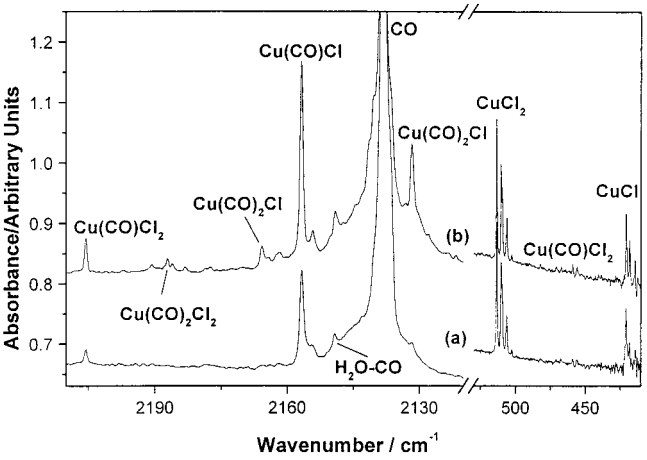

Figure 3. Infrared spectra in the 2210−2120 and 530−410 cm^{-1} regions from codeposition of laser-ablated $CuCl_2$ and 0.15% CO in argon: (a) 1 h sample deposition at 11 K; (b) after 30 K annealing.

sorptions (not shown).[27] Meanwhile, new absorptions at 2205.5, 2156.8, and 459.1 cm^{-1} were also observed on sample deposition. Annealing markedly increased the 2205.5, 2156.8, and 459.1 cm^{-1} bands and produced weak new bands at 2187.1, 2165.8, and 2131.6 cm^{-1}. Isotopic substitution experiments were also done, and the spectra are shown in Figure 4.

(c) CuCl + CO/Ar. Similar experiments were done using a CuCl target, and the spectra in the 2210−2120 cm^{-1} region are shown in Figure 5. Codeposition of laser-ablated CuCl with CO/Ar produced CuCl absorptions and the 2165.8, 2156.8, and 2131.6 cm^{-1} absorptions with approximately the same intensity as in the $CuCl_2$ + CO/Ar experiments, but the $CuCl_2$ absorptions and the 2205.5, 2187.1, and 459.1 cm^{-1} absorptions could hardly be observed.

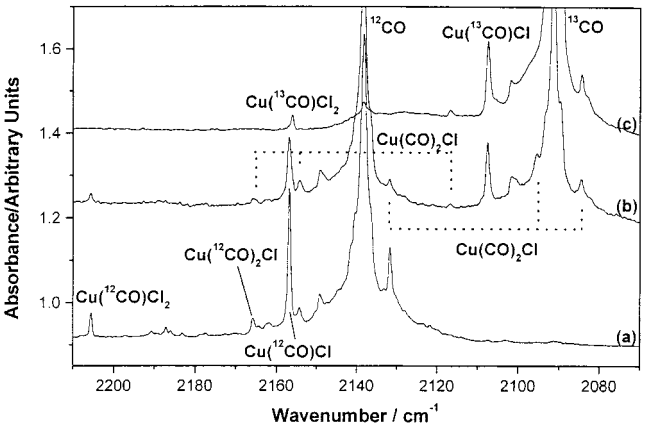

Figure 4. Infrared spectra in the 2210−2060 cm^{-1} region from codeposition of laser-ablated $CuCl_2$ and CO in excess argon: (a) 0.15% ^{12}CO, after 25 K annealing; (b) 0.1% ^{12}CO + 0.1% ^{13}CO, 25 K annealing; (c) 0.2% ^{13}CO, after 25 K annealing.

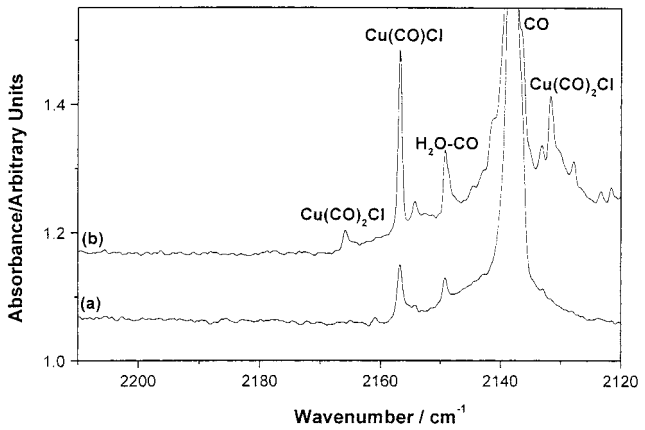

Figure 5. Infrared spectra in the 2210−2120 cm^{-1} region from codeposition of laser-ablated CuCl and 0.15% CO in argon: (a) 1 h sample deposition at 11 K; (b) after 30 K annealing.

(d) AgCl + CO/Ar. An AgCl target was also used in such experiments. The infrared spectra in the CO stretching vibrational region are presented in Figure 6. The observed band positions are listed in Table 3. Except for the $Ag(CO)_x$ absorptions,[28] one new absorption at 2184.0 cm^{-1} was observed; this band increased on annealing and was shifted to 2134.5 cm^{-1} with a $^{13}C^{16}O$ sample (trace d). In the mixed ^{12}CO + ^{13}CO spectrum (trace c), only pure isotopic counterparts were presented.

Calculation Results. DFT calculations were performed on the potential products observed in present experiments. The optimized geometric parameters for $M(CO)Cl$, $M(CO)_2Cl$, $M(CO)Cl_2$, and $M(CO)_2Cl_2$ (M = Ni, Cu, Ag) are shown in Figures 7 and 8, respectively. For comparison, the calculated geometric parameters for

(26) Martin, T. P.; Schaber, H. *J. Chem. Phys.* **1980**, *73*, 3541.
(27) Huber, H.; Kundig, E. P.; Moskovits, M.; Ozin, G. A. *J. Am. Chem. Soc.* **1975**, *97*, 2097.
(28) McIntosh, D.; Ozin, G. A. *J. Am. Chem. Soc.* **1976**, *98*, 3167.

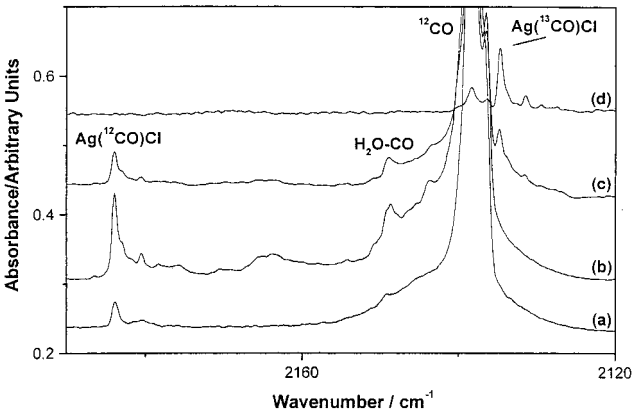

Figure 6. Infrared spectra in the 2200−2070 cm^{-1} region from codeposition of laser-ablated AgCl and CO in excess argon: (a) 0.15% ^{12}CO, 1 h sample deposition at 11 K; (b) after 30 K annealing; (c) 0.1% ^{12}CO + 0.1% ^{13}CO, after 30 K annealing; (d) 0.5% ^{13}CO, after 30 K annealing.

Table 3. IR Absorption (cm^{-1}) from Codeposition of Laser-Ablated AgCl with CO in Excess Argon at 11 K

$^{12}C^{16}O$	$^{13}C^{16}O$	*R*(12/13)	assignt
2184.0	2134.5	1.0232	Ag(CO)Cl
1958.6	1951.2	1.0227	Ag(CO)$_3$
1841.7	1800.7	1.0228	Ag(CO)$_2$

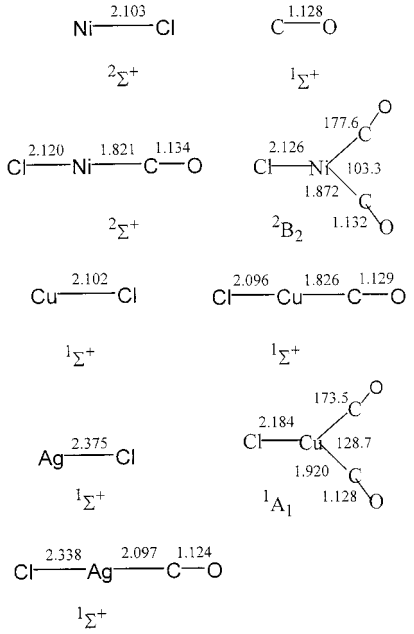

Figure 7. Calculated geometric parameters (bond lengths in angstroms, bond angles in degrees) of the M(CO)Cl and M(CO)$_2$Cl molecules.

CO, MCl, and MCl$_2$ are also shown in the figures. The calculated vibrational frequencies and intensities are listed in Tables 4 and 5.

Discussion

Ni(CO)Cl$_2$. DeKock et al. have deposited thermal evaporated NiCl$_2$ in CO-doped Ar and obtained two new absorptions at 2189 and 468 cm^{-1}. These two bands were assigned to the antisymmetric NiCl$_2$ and C−O stretching vibrations of the Ni(CO)Cl$_2$ molecule.[7,8] Similar absorptions at 2190.2 and 469.1 cm^{-1} were observed in our laser ablation experiments. The 2190.2 cm^{-1} band

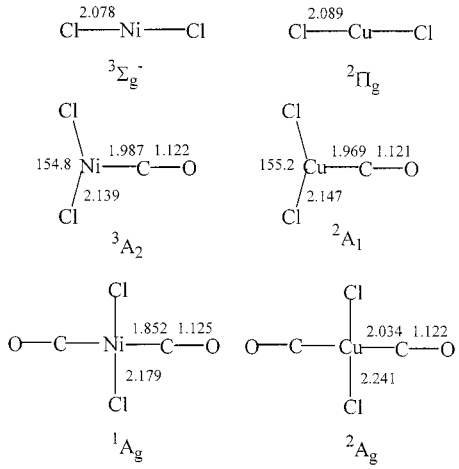

Figure 8. Calculated geometric parameters (bond lengths in angstroms, bond angles in degrees) of the M(CO)Cl$_2$ and M(CO)$_2$Cl$_2$ molecules.

Table 4. Calculated Vibrational Frequencies (cm^{-1}) and Intensities (km/mol, in Parentheses) of the M(CO)Cl (M = Ni, Cu, Ag) and M(CO)Cl$_2$ (M = Ni, Cu) Molecules

ClNiCO	ClCuCO	ClAgCO	Cl$_2$NiCO	Cl$_2$CuCO
2174 (713, σ)	2212 (595, σ)	2235 (459, σ)	2248 (291, a_1)	2262 (260, a_1)
502 (3, σ)	485 (1, σ)	341 (15, σ)	451 (120, b_2)	427 (82, b_2)
362 (1, π)	369 (2, π)	273 (2, π)	338 (3, a_1)	324 (1, a_1)
345 (53, σ)	345 (40, σ)	244 (26, σ)	329 (1, b_2)	311 (4, b_2)
71 (15, π)	78 (10, π)	57 (10, π)	277 (5, a_1)	291 (2, a_1)
			236 (1, b_1)	250 (2, b_1)
			104 (8, a_1)	97 (11, b_1)
			52 (0, b_2)	88 (8, a_1)
			51 (11, b_1)	38 (0, b_2)

Table 5. Calculated Vibrational Frequencies (cm^{-1}) and Intensities (km/mol, in Parentheses) of the M(CO)$_2$Cl and M(CO)$_2$Cl$_2$ Molecules (M = Ni, Cu)[a]

Ni(CO)$_2$Cl	Cu(CO)$_2$Cl	Ni(CO)$_2$Cl$_2$	Cu(CO)$_2$Cl$_2$
2192 (457, a_1)	2220 (204, a_1)	2250 (0, a_g)	2255 (0, a_g)
2149 (939, b_2)	2186 (868, b_2)	2219 (778, b_{1u})	2249 (440, b_{1u})
457 (1, a_1)	370 (18, a_1)	530 (57, b_{2u})	391 (75, b_{2u})
430 (13, a_1)	361 (8, b_2)	459 (8, b_{3u})	356 (0, b_{3g})
373 (39, b_2)	334 (6, a_1)	445 (0, b_{3g})	342 (7, b_{2u})
351 (3, b_1)	304 (2, b_1)	421 (72, b_{2u})	288 (0, a_g)
320 (46, a_1)	303 (17, a_1)	404 (18, b_{1u})	272 (1, b_{1u})
293 (2, b_2)	276 (20, b_2)	367 (0, a_g)	265 (2, b_{3u})
253 (0, a_2)	227 (0, a_2)	333 (0, b_{2g})	210 (0, b_{2g})
76 (4, b_1)	61 (4, b_1)	311 (0, a_g)	192 (0, a_g)

[a] Only the highest 10 vibrational frequencies are listed.

shifted to 2141.2 cm^{-1} with ^{13}CO, and no intermediate absorption was observed in the mixed ^{12}CO + ^{13}CO spectrum, indicating that only one CO is involved in this mode. DFT calculations predicted the Ni(CO)Cl$_2$ molecule to have a $^3A_2$ ground state with planar C_{2v} geometry. The NiCl$_2$ unit in Ni(CO)Cl$_2$ is slightly bent (154.8°), while NiCl$_2$ is linear. The C−O stretching and antisymmetric NiCl$_2$ stretching modes were predicted at 2248 and 450 cm^{-1}.

Ni(CO)Cl. Codeposition of laser-ablated NiCl$_2$ with CO in excess argon produced a new absorption at 2118.7 cm^{-1}. This band shifted to 2069.9 cm^{-1} with ^{13}CO and gave a ^{12}C/^{13}C ratio of 1.0236. Although the number of CO groups involved cannot be determined using a mixed ^{12}CO + ^{13}CO sample due to the strong absorptions of

Table 6. Scaling Factors and the Observed and Calculated Isotopic C−O Stretching Vibrational Frequency Ratios of the Observed Carbonyl Chloride Molecules

		$^{12}CO/^{13}CO$	
molecule	scaling factor	obsd	calcd
$Ni(CO)Cl_2$	0.974	1.0229	1.0231
Ni(CO)Cl	0.975	1.0236	1.0236
$Ni(CO)_2Cl$	0.970[a]	1.0231	1.0230
	0.966[b]	1.0226	1.0234
$Ni(CO)_2Cl_2$	0.968	1.0225	1.0231
$Cu(CO)Cl_2$	0.975	1.0230	1.0232
Cu(CO)Cl	0.975	1.0235	1.0236
$Cu(CO)_2Cl$	0.975[a]	1.0232	1.0235
	0.975[b]	1.0226	1.0230
$Cu(CO)_2Cl_2$	0.972		1.0231
Ag(CO)Cl	0.977	1.0232	1.0231

[a] Symmetric mode. [b] Antisymmetric mode.

^{13}CO, one CO unit is most probably involved in this mode, as the 2118.7 cm^{-1} band is the major product absorption observed on sample deposition in all experiments. This band increased on annealing in a lower CO concentration experiment but decreased on annealing in a higher CO concentration experiment. We know that laser ablation of the $NiCl_2$ target produces $NiCl_2$ as well as NiCl and Ni atoms. The 2118.7 cm^{-1} band was not observed either in thermal evaporated $NiCl_2$ + CO/Ar experiments or in laser-ablated Ni + CO/Ar experiments, suggesting that the 2118.7 cm^{-1} band is most probably due to the reaction product of NiCl and CO. Accordingly, the 2118.7 cm^{-1} band is assigned to the C−O stretching vibration of the Ni(CO)Cl molecule. The assignment is strongly supported by DFT calculations. As shown in Figure 7, the Ni(CO)Cl molecule was predicted to have a $^2\Sigma^+$ ground state with linear structure. The Ni−Cl, Ni−C, and C−O bond lengths were calculated to be 2.120, 1.821, and 1.134 Å, respectively. The C−O bond length is 0.006 Å longer than that of diatomic CO calculated at the same level. The C−O stretching vibration was predicted at 2174 cm^{-1}; we note that the vibrational fundamental of diatomic CO was calculated to be 2212 cm^{-1} at the same level. As listed in Table 6, the calculated isotopic frequency ratio is in excellent agreement with the observed value. The Ni−Cl stretching vibrational mode was calculated at 503 cm^{-1} with very low intensity and was not observed in the experiments.

$Ni(CO)_2Cl$. Weak bands at 2126.6 and 2075.0 cm^{-1} increased together on annealing. These two bands shifted to 2078.5 and 2029.1 cm^{-1} with ^{13}CO and gave $^{12}CO/^{13}CO$ isotopic ratios of 1.0231 and 1.0226. The 2075.0 cm^{-1} band formed triplets at 2075.0, 2042.7, and 2029.1 cm^{-1} with ^{12}CO + ^{13}CO, indicating that two equivalent CO groups are involved in this mode. These two bands are assigned to the symmetric and antisymmetric C−O stretching vibrations of the $Ni(CO)_2Cl$ molecule. DFT calculations predicted the $Ni(CO)_2Cl$ molecule to have a $^2B_2$ ground state with symmetric and antisymmetric C−O stretching vibrations at 2192 and 2149 cm^{-1}, which require scaling factors of 0.970 and 0.966 to fit the experimental frequencies.

$Ni(CO)_2Cl_2$. The 2148.4 cm^{-1} band appeared only on annealing. It was partially overlapped by the H_2O−CO absorption at 2149.2 cm^{-1} and may be due to alternations of the site of the H_2O−CO. However, no such alterations were observed in the $CuCl_2$ and AgCl experiments, suggesting that the 2148.4 cm^{-1} band is not due to the site of H_2O−CO. The 2148.4 cm^{-1} absorption shifted to 2101.2 cm^{-1} with ^{13}CO and defines a $^{12}CO/^{13}CO$ ratio of 1.0225, indicating a C−O stretching vibration. This band appeared only on annealing, suggesting more than one CO involvement. In the low-frequency region, two weak bands at 525.2 and 434.4 cm^{-1} went together with the 2148.4 cm^{-1} band, suggesting different modes of the same molecule. The 434.4 cm^{-1} band can be assigned to an antisymmetric $NiCl_2$ stretching vibration from its isotopic structure. These three bands are assigned to the $Ni(CO)_2Cl_2$ molecule. The 525.2 cm^{-1} band is due to in-plane NiCO bending mode. The two low-frequency modes have been reported at 522.8 and 428.2 cm^{-1} in solid CO,[9] which are in good agreement with our argon matrix values. As shown in Figure 8, the $Ni(CO)_2Cl_2$ molecule was calculated to have a ^1A_g ground state with planar D_{2h} symmetry. The antisymmetric C−O stretching (B_{1u}), in-plane NiCO bending (b_{2u}), and antisymmetric $NiCl_2$ stretching (b_{2u}) vibrational frequencies were predicted at 2219, 530, and 421 cm^{-1}, respectively, with 778:57:72 relative intensities.

Cu(CO)Cl. The 2156.8 cm^{-1} band is the major product absorption in experiments with $CuCl_2$ and CuCl targets. It shifted to 2107.3 cm^{-1} with ^{13}CO and gave a $^{12}CO/^{13}CO$ isotopic ratio of 1.0235. A doublet isotopic structure was presented in the mixed ^{12}CO + ^{13}CO spectrum, which indicated one CO involvement. This band is assigned to the C−O stretching vibration of the Cu(CO)Cl molecule. As shown in Figure 7, the Cu(CO)Cl molecule was predicted to have a $^1\Sigma^+$ ground state with linear geometry. The C−O stretching vibration was calculated at 2112 cm^{-1}, which requires a scaling factor of 0.975 to fit the observed value. This scaling factor is the same as that of the Ni(CO)Cl and $Ni(CO)Cl_2$ molecule. The calculated $^{12}CO/^{13}CO$ isotopic ratio of 1.0236 is about the same as the experimental value. As listed in Table 4, the CO stretching vibrational mode was predicted to be the most intense mode of the Cu(CO)Cl molecule.

The solid-state Cu(CO)Cl has been prepared by passing carbon monoxide through the copper chloride solution, and the crystal structure has been characterized.[6] The solid Cu(CO)Cl contains chloride-bridged layers in which copper is approximately tetrahedrally coordinated; the Cu−C and C−O distances were determined to be 1.86 and 1.11 Å. These two bond distances of the isolated Cu(CO)Cl molecule were calculated to be 1.826 and 1.129 Å, close to the solid values.

$Cu(CO)Cl_2$. The 2205.5 and 459.1 cm^{-1} absorptions increased together on annealing in $CuCl_2$ + CO/Ar experiments. These two bands were not observed in CuCl + CO/Ar experiments, suggesting that these two bands be due to the reaction product of $CuCl_2$ and CO. The 459.1 cm^{-1} band showed no ^{13}CO isotopic shift and can be assigned to an antisymmetric $CuCl_2$ stretching vibration. The 2205.5 cm^{-1} band shifted to 2156.0 cm^{-1} with ^{13}CO, and no obvious intermediate was observed in the mixed ^{12}CO + ^{13}CO spectrum; therefore, one CO is most probably involved in this mode. These two bands are assigned to the $Cu(CO)Cl_2$ molecule following the $Ni(CO)Cl_2$ example. DFT calculations predicted that Cu-

$(CO)Cl_2$ has a $^2A_1$ ground state with planar C_{2v} geometry. The CO stretching and antisymmetric $CuCl_2$ stretching vibrational modes were predicted at 2262 and 427 cm^{-1} with 260:82 relative intensities. The 2205.5 cm^{-1} CO stretching vibrational frequency is the highest ever reported for the first-row transition-metal monocarbonyl dichlorides.[7]

$Cu(CO)_2Cl$. The 2165.8 and 2131.6 cm^{-1} bands increased together on annealing, suggesting different vibrational modes of the same molecule. These two bands were observed in both $CuCl_2$ + CO/Ar and CuCl + CO/Ar experiments, and the intensities are about the same in both experiments, which suggest that one CuCl unit is most probably involved in this molecule. These two bands shifted to 2116.7 and 2084.4 cm^{-1} with ^{13}CO and gave $^{12}CO/^{13}CO$ isotopic ratios of 1.0232 and 1.0226. The isotopic ratio of the upper mode is slightly higher than that of the lower mode, indicating more C involvement in the upper mode than the lower mode. Both bands formed triplets at 2165.8, 2154.3, and 2116.7 cm^{-1} and 2131.6, 2095.4, and 2084.4 cm^{-1} with $^{12}CO + {}^{13}CO$, indicating that two equivalent CO molecules are involved in these two modes. These two bands are assigned to the symmetric and antisymmetric C−O stretching vibrations of the $Cu(CO)_2Cl$ molecule. The assignment is further confirmed by DFT calculations. As shown in Figure 7, the $Cu(CO)_2Cl$ molecule was predicted to have a $^1A_1$ ground state with C_{2v} symmetry. The symmetric and antisymmetric C−O stretching vibrational modes were calculated to be 2220 and 2186 cm^{-1} with 204:868 relative intensities. As listed in Table 6, the calculated isotopic ratios are in good agreement with the experimental values.

$Cu(CO)_2Cl_2$. Weak bands around 2178.1 cm^{-1} were only observed in the $CuCl_2$ + CO/Ar experiment on high-temperature annealing, suggesting that these bands are due to cluster species. The most intense 2178.1 cm^{-1} band is probably due to the antisymmetric C−O stretching vibration of the $Cu(CO)_2Cl_2$ molecule. As shown in Figure 8, this molecule was predicted to have a ^2A_g ground state with planar D_{2h} symmetry, with a strong antisymmetric C−O stretching vibration at 2249 cm^{-1}.

Ag(CO)Cl. The 2184.0 cm^{-1} band is the only new product absorption in the AgCl + CO/Ar experiments. This band was observed after sample deposition and increased on annealing. It shifted to 2134.5 cm^{-1} with a ^{13}CO sample. The $^{12}CO/^{13}CO$ ratio 1.0232 indicates that it is a carbonyl stretching vibration, and the mixed $^{12}CO + {}^{13}CO$ spectrum confirmed one CO involvement. This band is assigned to the Ag(CO)Cl molecule. Our DFT calculations characterized this Ag(CO)Cl molecule with linear geometry and a $^1\Sigma^+$ ground state (Figure 7). The predicted C−O stretching vibrational frequency is 2235 cm^{-1}, and the $^{12}CO/^{13}CO$ isotopic ratio is 1.0231. This frequency requires a 0.977 scaling factor.

Silver is probably the only transition metal that failed to form stable monocarbonyl. Although earlier researchers claimed the existence of the silver monocarbonyl in rare-gas matrices,[28] no evidence of the isolated silver monocarbonyl was found in later experiments.[29,30] The matrix ESR and theoretical studies showed that silver monocarbonyl is not a stable complex.[29] Hurlburt et al. synthesized the first isolable silver monocarbonyl complex, $Ag(CO)B(OTeF_5)_4$, by reacting the extremely hygroscopic compounds $AgOTeF_5$ and $AgB(OTeF_5)_4$ with a CO atmosphere.[31] The solid-state IR spectrum of $Ag(CO)B(OTeF_5)_4$ exhibited a CO stretching vibrational frequency at 2204 cm^{-1}, 20 cm^{-1} higher than that of the Ag(CO)Cl. Recently, the $AgCO^+$ cation has been formed and identified in solid neon; the C−O stretching frequency was observed at 2233.1 cm^{-1}.[30]

In our AgCl + CO/Ar experiments, no evidence was found for the $Ag(CO)_2Cl$ molecule. Our DFT calculations found a stable minimum for the $Ag(CO)_2Cl$ molecue; however, this stable minimum is higher in energy than Ag(CO)Cl + CO. Silver dicarbonyl, $Ag(CO)_2$, is a stable molecule and can be formed by reaction of a silver atom and CO. The dicarbonyl complex $Ag(CO)_2[B(OTeF_5)_4]$ as a crystalline solid has also been synthesized; this compound lost one CO under vacuum, leaving $Ag(CO)B(OTeF_5)_4$.[31] This may suggest that $Ag(CO)_2[B(OTeF_5)_4]$ is also less stable than $Ag(CO)B(OTeF_5)_4$.

In the MCl molecules, there is partial positive charge on the metal center; therefore, the M(CO)Cl molecules can be viewed as CO binding to a partially charged metal center, and the bonding mechanism will be very similar to the MCO^+ cations, the bonding mechanism of which has been well discussed.[32−34] Table 7 lists the binding energies of the carbonyl chlorides calculated at the B3LYP level. For comparison, the calculated and experimental binding energies of monocarbonyl neutrals and cations are also listed. Recent studies have shown that the B3LYP hybrid functional can provide very reliable predictions of the binding energies of transition-metal-containing compounds.[15−17] As can be seen from Table 7, B3LYP calculations predicted the binding energies of $NiCO^+$, CuCO, $CuCO^+$, and $AgCO^+$ quite well.[35−38] The large difference between calculated and experimental binding energies of NiCO is due to the dif-

Table 7. Calculated Binding Energies (D_e, kcal/mol) of the ClMCO and Cl_2MCO Molecules (M = Ni, Cu, Ag) with Respect to MCl + CO or MCl_2 + CO[a]

molecule	calcd[b]	exptl
Cl_2NiCO	11.0	
ClNiCO	37.7	
Cl_2CuCO	8.7	
ClCuCO	34.2	
ClAgCO	17.8	
NiCO	31.6	40.5 ± 5.8[c]
CuCO	7.4	6−8[d]
$NiCO^+$	38.9	41.7 ± 2.5[e]
$CuCO^+$	34.8	35.5 ± 1.6[f]
$AgCO^+$	20.6	21.2 ± 1.2[f]

[a] For comparison, the calculated and experimental binding energies of monocarbonyl neutral species and cations are also listed. [b] Binding energies are corrected with zero point energy (ZPE), this work. [c] Reference 35. [d] Reference 36. [e] Reference 37. [f] Reference 38.

(29) Kasai, P. H.; Jones, P. M. *J. Phys. Chem.* **1985**, *89*, 1147.
(30) Liang, B. Y.; Andrews, L. *J. Phys. Chem. A*, in press.
(31) Hurlburt, P. K.; Anderson, O. P.; Strauss, S. H. *J. Am. Chem. Soc.* **1991**, *113*, 6277. Hurlburt, P. K.; Rack, J. J.; Luck, J. S.; Dec, S. F.; Webb, J. D.; Anderson, O. P.; Strauss, S. H. *J. Am. Chem. Soc.* **1994**, *116*, 10003.
(32) Barnes, L. A.; Rosi, M.; Bauschlicher, C. W., Jr. *J. Chem. Phys.* **1990**, *93*, 609. Bauschlicher, C. W., Jr. *J. Chem. Phys.* **1986**, *84*, 260.
(33) Blomberg, M.; Brandemark, U.; Johansson, J.; Siegbahn, P.; Wennerberg, J. *J. Chem. Phys.* **1988**, *88*, 4324. Mavridis, A.; Harrison, J. F.; Allison, J. *J. Am. Chem. Soc.* **1989**, *111*, 2482.
(34) Veldkamp, A.; Frenking, G. *Organometallics* **1993**, *12*, 4613. Ehlers, A. W.; Ruiz-Morales, Y.; Baerends, E. J.; Ziegler, T. *Inorg. Chem.* **1997**, *36*, 5031.

ficult prediction of atomic Ni by DFT calculations. The binding energies of Ni(CO)Cl, Cu(CO)Cl, and Ag(CO)Cl were predicted to be 37.7, 34.2, and 17.8 kcal/mol, respectively, after zero point energy corrections. These values are slightly smaller than those of the MCO^+ cations. The binding energies of $Ni(CO)Cl_2$ and $Cu(CO)Cl_2$ were calculated to be 11.0 and 8.7 kcal/mol, significantly lower than those of the Ni(CO)Cl and Cu(CO)Cl molecules.

Thermal evaporation of MCl_2 could only produce MCl_2 molecules. Because of the easy formation of clusters, it was difficult to obtain CuCl in a matrix via thermal evaporation of solid CuCl.[39] However, laser ablation of MCl_2 targets produces MCl_2 as well as MCl; it is easy to produce and isolate the MCl in argon using laser ablation, and the M(CO)Cl species were produced via reactions 1−3, which were predicted to be exothermic. In lower CO concentration experiments, the M(CO)Cl absorptions increased on annealing, suggesting that reactions 1−3 require negligible activation energy. The Ni(CO)Cl and Cu(CO)Cl can further react with CO to form $Ni(CO)_2Cl$ and $Cu(CO)_2Cl$, via reactions 4 and 5.

$$NiCl\ (^2\Sigma^+) + CO \rightarrow Ni(CO)Cl\ (^2\Sigma^+) \qquad \Delta E = -37.7\ \text{kcal/mol} \quad (1)$$

$$CuCl\ (^1\Sigma^+) + CO \rightarrow Cu(CO)Cl\ (^1\Sigma^+) \qquad \Delta E = -34.2\ \text{kcal/mol} \quad (2)$$

$$AgCl\ (^1\Sigma^+) + CO \rightarrow Ag(CO)Cl\ (^1\Sigma^+) \qquad \Delta E = -17.8\ \text{kcal/mol} \quad (3)$$

$$Ni(CO)Cl\ (^2\Sigma^+) + CO \rightarrow Ni(CO)_2Cl\ (^2B_2) \qquad \Delta E = -18.6\ \text{kcal/mol} \quad (4)$$

$$Cu(CO)Cl\ (^1\Sigma^+) + CO \rightarrow Cu(CO)_2Cl\ (^1A_1) \qquad \Delta E = -2.7\ \text{kcal/mol} \quad (5)$$

In the $NiCl_2$ + CO and $CuCl_2$ + CO reactions, the $M(CO)Cl_2$ species were produced on deposition and the $M(CO)_2Cl_2$ species appeared on annealing. These molecules were formed by MCl_2 and CO reactions:

$$NiCl_2\ (^3\Sigma_g^-) + CO \rightarrow Ni(CO)Cl_2\ (^3A_2) \qquad \Delta E = -11.0\text{kcal/mol} \quad (6)$$

$$CuCl_2\ (^2\Pi_g) + CO \rightarrow Cu(CO)Cl_2\ (^2A_1) \qquad \Delta E = -8.7\text{kcal/mol} \quad (7)$$

$$Ni(CO)Cl_2\ (^3A_2) + CO \rightarrow Ni(CO)_2Cl_2\ (^1A_g) \qquad \Delta E = -13.1\text{kcal/mol} \quad (8)$$

$$Cu(CO)Cl_2\ (^2A_1) + CO \rightarrow Cu(CO)_2Cl_2\ (^2A_g) \qquad \Delta E = -5.0\text{kcal/mol} \quad (9)$$

Conclusions

Laser-ablated nickel, copper, and silver chlorides reacted with CO in excess argon to give the monocarbonyl chlorides M(CO)Cl (M = Ni, Cu, Ag) and $M(CO)Cl_2$ (M = Ni, Cu). Through annealing, the dicarbonyl chlorides $M(CO)_2Cl$ and $M(CO)_2Cl_2$ (M = Ni, Cu) were produced and identified.

DFT calculations have been performed for all products. The excellent agreement between experimental results with the frequencies and isotopic frequency ratios from density functional calculations support the vibrational assignments and the identification of these metal carbonyl chloride complexes. As listed in Table 6, the scaling factors for the C−O stretching vibrational modes are within the range 0.968−0.977. The M(CO)Cl molecules (M = Ni, Cu, Ag) were predicted to have linear structures, and the binding energies with respect to MCl + CO were estimated to be 37.7, 34.2, and 17.8 kcal/mol, respectively. These simple transition-metal carbonyl chloride complexes could serve as model compounds for this class of complexes.

Acknowledgment. We gratefully acknowledge support from the NSFC (Grant No. 20003003) and the Chinese NKBRSF and Mr. J. Dong and H. Lu for some experimental work.

OM000911H

(35) Sunderlin, L. S.; Wang, D.; Squires, R. R. *J. Am. Chem. Soc.* **1992**, *114*, 2788.
(36) Blitz, M. A.; Mitchell, S. A.; Hackett, P. A. *J. Phys. Chem.* **1991**, *95*, 8719.
(37) Khan, F. A.; Steele, D. L.; Armentrout, P. B. *J. Phys. Chem.* **1995**, *99*, 7819.
(38) Meyer, F.; Chen, Y.; Armentrout, P. B. *J. Am. Chem. Soc.* **1995**, *117*, 4071.
(39) Plitt, H. S.; Bar, M. R.; Ahlrichs, R.; Schnockel, H. *Angew. Chem., Int. Ed. Engl.* **1991**, *30*, 832.